Photoacoustics 48 (2026) 100811

Contents lists available at ScienceDirect

Photoacoustics

journal homepage: www.elsevier.com/locate/pacs

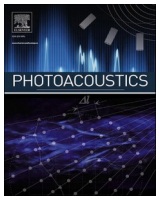

Letter to the Editor

Spatially engineered optical–acoustic matching in quartz-enhanced photoacoustic spectroscopy

ARTICLE INFO

Keywords:
Quartz-enhanced photoacoustic spectroscopy
Conical acoustic collector
Multi-pass cell
Quartz tuning fork

ABSTRACT

Quartz-enhanced photoacoustic spectroscopy (QEPAS) offers high sensitivity for trace-gas detection, but its performance is often limited by a spatial mismatch between distributed photoacoustic excitation and the intrinsic sensitivity region of the quartz tuning fork (QTF). In many multi-pass QEPAS configurations, extending the optical path length alone does not ensure efficient signal enhancement. Here, we present a spatially engineered optical–acoustic matching strategy for QEPAS. A confocal-like multi-pass cell folds the excitation beam multiple times while spatially confining optical absorption within the intrinsic high-sensitivity region of the QTF. In parallel, non-resonant conical acoustic collectors (CACs) geometrically match and efficiently collect the resulting distributed photoacoustic waves. Experimental validation using water vapor detection demonstrates an approximately 42-fold signal enhancement compared with a conventional single-pass QEPAS configuration under identical conditions. The enhancement is achieved without relying on narrowband acoustic resonance or stringent optical alignment, establishing spatial engineering as a robust and general framework for improving QEPAS performance.

1. Introduction

Photoacoustic spectroscopy (PAS) has emerged as a powerful technique for trace-gas detection owing to its capability to directly convert absorbed optical energy into acoustic signals [1–17]. Among various PAS implementations, quartz-enhanced photoacoustic spectroscopy (QEPAS) employs a quartz tuning fork (QTF) as a high-Q piezoelectric acoustic transducer, offering intrinsic advantages including compactness, strong immunity to environmental noise, and high detection sensitivity [18–25]. These features make QEPAS particularly attractive for portable and field-deployable gas-sensing applications. Consequently, substantial efforts have been devoted over the past decade to further improving the sensitivity of QEPAS-based sensors [26–28].

Most reported QEPAS enhancement strategies can be broadly classified into two categories: acoustic-field enhancement and optical-excitation enhancement. Acoustic-field enhancement typically relies on auxiliary resonant structure, such as micro-resonators or acoustic tubes placed near the QTF, to increase sound-energy coupling efficiency [29–32]. Optical enhancement, on the other hand, aims to increase the absorbed optical energy by extending the effective light–matter interaction length, for example through multi-pass or multi-beam excitation schemes. While these approaches have demonstrated notable signal improvements, they predominantly focus on increasing either acoustic resonance strength on optical path length [33–36]. In addition, alternative QEPAS transduction schemes have been explored recently, for example through optical readout of the quartz tuning fork, further reflecting ongoing efforts to enhance QEPAS sensitivity [37,38].

However, a fundamental aspect that has received far less attention in existing QEPAS enhancement schemes is the intrinsic spatial response characteristics of the QTF, which governs how efficiently photoacoustic waves generated at different spatial locations are transduced into an electrical signal. In many multi-pass QEPAS (MP-QEPAS) configurations, optical absorption occurs over an extended spatial region that only partially overlaps with this intrinsic sensitivity zone. As a result, a significant fraction of the generated photoacoustic waves is produced outside the effective detection region and dissipates before being efficiently transduced by the QTF, fundamentally limiting the achievable signal enhancement. As a consequence, increasing optical path length alone does not necessarily translate into proportional signal enhancement, revealing a fundamental limitation of many MP-QEPAS configurations.

Recent optical-excitation enhancement schemes, such as MP-QEPAS [36] and dual-antinode excitation [39], exemplify this limitation. Although multiple excitation beams are introduced, their spatial distribution is often dictated by optical folding constraints rather than by the QTF's acoustic response profile. Similarly, conventional cylindrical acoustic resonators are primarily designed for localized or quasi-point acoustic sources and exhibit poor geometric compatibility with the distributed, fan-shaped photoacoustic sources generated by multi-pass excitation. This spatial mismatch between optical excitation, acoustic wave generation, and QTF sensitivity represents a key bottleneck for further performance improvement.

In this work, we address this challenge by spatially engineering the optical excitation and acoustic collection to match the intrinsic spatial response of the QTF. The central idea is not to maximize optical or acoustic enhancement independently, but to maximize the effective spatial overlap between the distributed photoacoustic source volume and the intrinsic sensitivity region of the QTF. A confocal-like multi-pass cell (MPC) is designed to fold the excitation beam multiple times while tightly confining all optical trajectories within the QTF's high-sensitivity region. This ensures that virtually all photoacoustic sources contribute effectively to the QTF response. In parallel, a pair of non-resonant conical acoustic collectors (CACs) is introduced to geometrically match the spatial distribution of the distributed photoacoustic sources

https://doi.org/10.1016/j.pacs.2026.100811

Available online 17 February 2026

produced by the multi-pass excitation. Unlike conventional cylindrical resonators, the CACs function as broadband acoustic funnels that efficiently collect and guide sound energy toward the QTF without imposing stringent resonance-matching or alignment requirements. Through this coordinated optical–acoustic spatial matching, substantial signal enhancement is achieved while maintaining system robustness and experimental simplicity. The proposed approach is experimentally validated using trace-gas detection under ambient conditions, demonstrating its potential as a robust and general route for enhancing QEPAS performance.

2. Principle and design

2.1. Spatially confined multi-pass optical excitation

To maximize the effective contribution of optical excitation to the QTF response, the optical field must be spatially confined within the intrinsic high-sensitivity region of the QTF rather than merely extended along the optical path. Unlike conventional multi-pass QEPAS configurations, which primarily aim at increasing the optical path length, the MPC in this work is deliberately designed to control the spatial distribution of optical absorption. The key objective is to ensure that all folded excitation beams generate photoacoustic sources entirely inside the QTF effective response region, thereby maximizing the transduction efficiency of each excitation pass. To this end, a near-confocal multi-pass optical configuration is employed to produce a fan-shaped beam distribution that converges within a well-defined spatial region matched to the QTF sensitivity profile. Ray-tracing simulations are used as a practical tool to identify representative optical parameters that simultaneously satisfy multi-pass stability and spatial confinement requirements.

The MPC consists of two identical spherical concave mirrors (Mirror I and Mirror II) [40,41], mounted on parallel cage plates connected by rigid cage rods. This configuration allows precise adjustment of the mirror separation distance d, which governs the stability and folding behavior of the optical trajectories. A collimated excitation beam is injected into the MPC with finite angular components along both the y- and z-axes, where the z-axis coincides with the MPC optical axis and the y-axis is aligned with the symmetry axis of the QTF. By carefully selecting the injection position and angle, the beam undergoes multiple reflections between the two mirrors, forming a stable and reproducible multi-pass trajectory. Importantly, the MPC is not designed solely to increase optical path length. Instead, the optical parameters are chosen to satisfy the near-confocal stability condition $4f/d \approx 1$, where f is the mirror focal length. Under this condition, the folded beams form a symmetric, fan-shaped distribution in the y–z plane, while the corresponding reflection spots appear as a linear array on the mirror surfaces. This geometric folding behavior enables controlled convergence of all excitation beams within a well-defined spatial region.

As illustrated in Fig. 1, the fan-shaped beam bundle converges within the QTF prong gap and is tightly confined to the QTF's intrinsic high-sensitivity region. The vertical extent of the convergence region, denoted by D, is governed by the geometry of the folded trajectories and satisfies the constraint:

$$D \leq |L_1 - L_2|$$

where L_1 and L_2 represent the distances from the upper and lower boundaries of the QTF optimal response region to the top of the QTF, respectively. This condition ensures that all folded beams generate photoacoustic excitation within the effective detection zone of the QTF, thereby maximizing the utilization of the QTF spatial response function. To avoid optical clipping, the QTF prong spacing is chosen to be larger than the beam diameter, allowing loss-free transmission of all folded beams through the prong gap.

The optical propagation within the MPC was first analyzed using ray-tracing simulations (TracePro) to identify representative multi-pass configurations that simultaneously satisfy stability and spatial confinement requirement. One optimized configuration employs two mirrors with a focal length of 25 mm and a diameter of 25.4 mm, separated by approximately 98.1 mm. In this case, the excitation beam is injected with a lateral offset of 13.45 mm and an incidence angle of -15.4° in the $y-z$ plane, resulting in more than 20 reflections within the MPC while maintaining tight spatial confinement of the beam convergence region. It should be noted that this parameter set is not unique. Owing to the geometric nature of the confinement mechanism, a range of injection positions and angles can yield similar fan-shaped folding patterns with comparable convergence characteristics. Therefore, the simulated parameters serve as practical guidelines for experimental alignment rather than strict design constraints. This tolerance highlights the robustness of the spatially confined multi-pass excitation scheme and its suitability for practical QEPAS implementations.

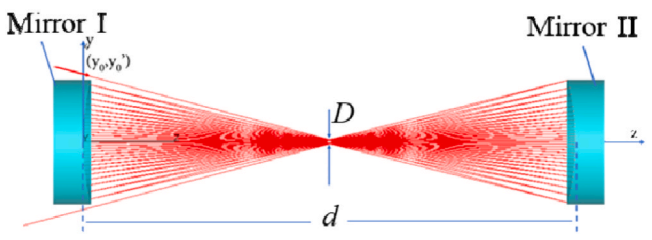

Fig. 1. Simulated fan-shaped optical trajectories in the y–z plane, illustrating the spatially confined multi-pass excitation. All folded sub-beams converge within the intrinsic high-sensitivity region of the QTF, ensuring that photoacoustic excitation occurs entirely inside the QTF prong gap.

2.2. Geometry-matched conical acoustic collectors for distributed sound-energy collection

While the spatially confined multi-pass optical excitation ensures that photoacoustic waves are generated predominantly within the intrinsic high-sensitivity region of the QTF, the resulting acoustic field is inherently distributed in space due to the presence of multiple excitation beams. Efficient transduction of this distributed acoustic energy therefore requires an acoustic collection scheme that is geometrically compatible with the spatial distribution of the photoacoustic sources, rather than one optimized for localized or quasi-point sources.

To address this requirement, a pair of identical CACs was designed and symmetrically positioned on both sides of the QTF along the optical axis. In contrast to conventional cylindrical acoustic resonators [32], which are primarily tailored to enhance specific resonance modes for localized excitation, the conical geometry provides a gradual spatial compression of sound energy, enabling efficient collection of acoustic waves generated over an extended region. This geometric feature makes the CACs particularly suitable for the fan-shaped distribution of photoacoustic sources produced by the spatially confined multi-pass excitation.

The dimensions of the CACs were determined based on the spatial characteristics of the folded optical trajectories, including the beam offset, incidence angle, and convergence height. The entrance aperture of each CAC was chosen to fully accommodate the spatial extent of the distributed acoustic sources, while the tapering profile guides the acoustic waves toward the QTF prong gap with minimal reflection loss. As a result, the CACs function as broadband acoustic energy collectors, rather than frequency-selective resonators, and do not impose stringent resonance-matching conditions on the QTF, since no sharp resonance is involved and any geometry-induced frequency dependence is expected to be weak and smooth.

Finite-element simulations were performed using COMSOL Multiphysics to evaluate the effectiveness of the conical collectors in concentrating distributed acoustic energy near the QTF. In the

simulations, multiple line acoustic sources were introduced to emulate the spatially distributed photoacoustic excitation generated by the multi-pass optical field. This line-source model is an idealized representation of slender finite-volume photoacoustic sources. Using a finite source volume would mainly smooth local near-field features and is not expected to change the qualitative comparison between different collector geometries under identical distributed excitation. For comparison, a cylindrical acoustic cavity with the same entrance diameter was also simulated. The results, shown in Fig. 2, indicate that each CAC produces a significantly higher sound-pressure concentration in the vicinity of the QTF prong gap, confirming its superior geometric compatibility with distributed acoustic sources. In addition to the field distributions shown in Fig. 2, quantitative analysis of the simulated axial acoustic pressure indicates that, at the QTF position, the peak pressure obtained with the CACs is approximately two times higher than that achieved with conventional cylindrical cavities of comparable size. Based on the simulation results, each CAC was fabricated as a truncated cone with an upper radius of 1.6 mm, a lower radius of 13 mm, and a height of 50 mm. The collectors were symmetrically aligned with respect to the QTF, with their narrow ends centered on the QTF prong gap. This geometry-matched acoustic collection scheme ensures that the spatially distributed photoacoustic waves generated by the confined multi-pass excitation are efficiently guided toward the region where the QTF exhibits maximum sensitivity.

3. Experimental setup

Based on the spatially engineered optical and acoustic design, described above, an experimental QEPAS system was constructed to validate the proposed optical-acoustic matching strategy. A schematic of the experimental setup is shown in Fig. 3. Water vapor (H_2O) was selected as the target analyte; accordingly, a distributed-feedback (DFB) laser operating at a wavelength of 1.395 μm with an output power of 16 mW was used as the excitation source. The laser was driven by a control electronics unit (CEU) and wavelength-modulated at half of the QTF resonance frequency to enable second-harmonic ($2f$) detection. The laser beam was collimated and injected into the MPC consisting of two spherical concave mirrors with a diameter of 25.4 mm and a focal length of 25 mm, mounted on a rigid cage structure. During alignment, the beam injection position and angle were finely adjusted around the simulated values to achieve stable multi-pass operation while ensuring that the folded beams converged within the predefined spatial region corresponding to the QTF intrinsic sensitivity zone. A reproducible multi-pass configuration with approximately 20 reflections was obtained, as confirmed by the experimentally observed reflection-spot pattern on the mirror surfaces and the corresponding photograph of the MPC shown in Fig. 3. The convergence height of the folded-beam envelope was on the order of 3 mm and showed a small alignment-dependent variation. In practice, the injection parameters were adjusted to maximize the overlap between the multi-pass excitation and the high-response zone defined in Fig. 5 while maintaining loss-free transmission through the prong gap.

A custom QTF with a prong length of 10 mm and a prong spacing of 800 μm was positioned at the center of the MPC. The prong spacing was chosen to be sufficiently larger than the laser beam diameter to ensure loss-free transmission of all folded beams through the QTF gap. Two CACs, fabricated from 100-μm-thick stainless steel with polished inner-wall surfaces, were symmetrically positioned on both sides of the QTF along the optical axis to collect and guide the distributed photoacoustic waves toward the QTF. The CACs were mechanically fixed by a circular-arc support underneath to ensure stable and reproducible alignment, with the collector apices centered on the QTF prong gap. Prior to gas-sensing measurements, the resonance characteristics of the QTF were experimentally characterized by electrical frequency sweeping. The measured resonance frequency was 7.209 kHz, and a Lorentzian fit yielded a quality factor of approximately 8500 under atmospheric conditions, as shown in Fig. 4. The photoacoustic signal generated by the QTF was amplified using a low-noise transimpedance preamplifier and subsequently demodulated by a lock-in amplifier. The demodulated signal was recorded for further analysis.

4. Results and discussion

The performance of the spatially engineered QEPAS system was experimentally evaluated under ambient laboratory conditions at room temperature and atmospheric pressure. Water vapor (H_2O) was selected as the target analyte, and the excitation wavelength was tuned to the absorption line centered at 7181 cm^{-1}.

Before evaluating the enhancement mechanisms, the intrinsic spatial response of the QTF was experimentally characterized using a conventional single-beam QEPAS configuration. The excitation beam was vertically scanned along the y-axis of the QTF from the prong tips (point a) toward the prong base (point b), while all other experimental parameters were kept constant. The normalized QEPAS signal as a function of beam position is shown in Fig. 5. A well-defined high-sensitivity region is observed along the prong length. Although the maximum response occurs approximately 1.2 mm below the prong tips, the high-response zone, defined here as positions where the signal remains above ~80 % of its peak value, spans about 2.8 mm along the prong length. This result indicates that the custom QTF exhibits a finite-width spatial sensitivity profile with a well-defined maximum, rather than an idealized point-like response. From a physical perspective, this spatial response profile reflects the modal displacement distribution of the QTF prongs and defines the effective region where photoacoustic excitation can be most efficiently transduced into an electrical signal. This experimentally determined spatial response function provides a critical design

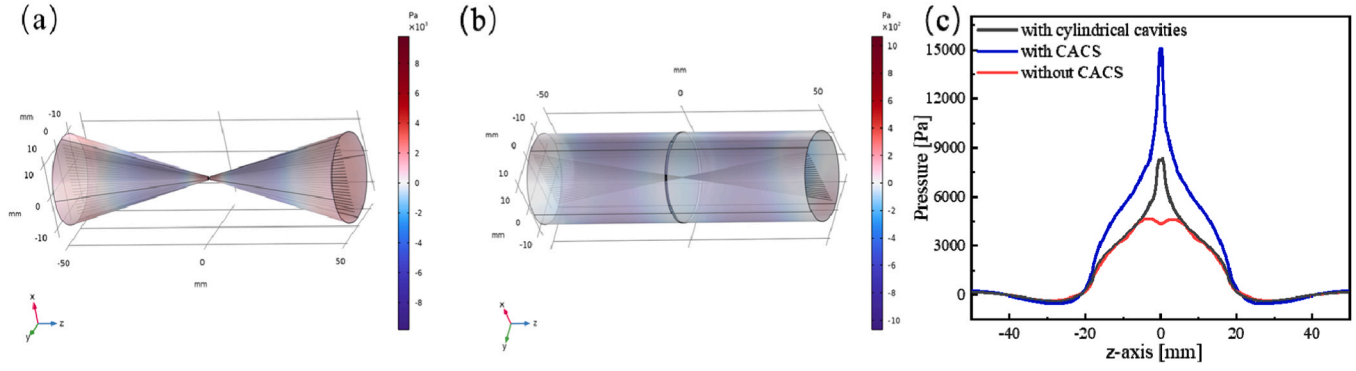

Fig. 2. COMSOL-simulated sound pressure distributions for (a) conical and (b) cylindrical acoustic collectors under fan-shaped, spatially distributed acoustic sources generated by the multi-pass excitation. (c) Simulated acoustic pressure along the z-axis (optical axis) for the two geometries. The conical geometry provides more effective geometric concentration of acoustic energy toward the collector apex.

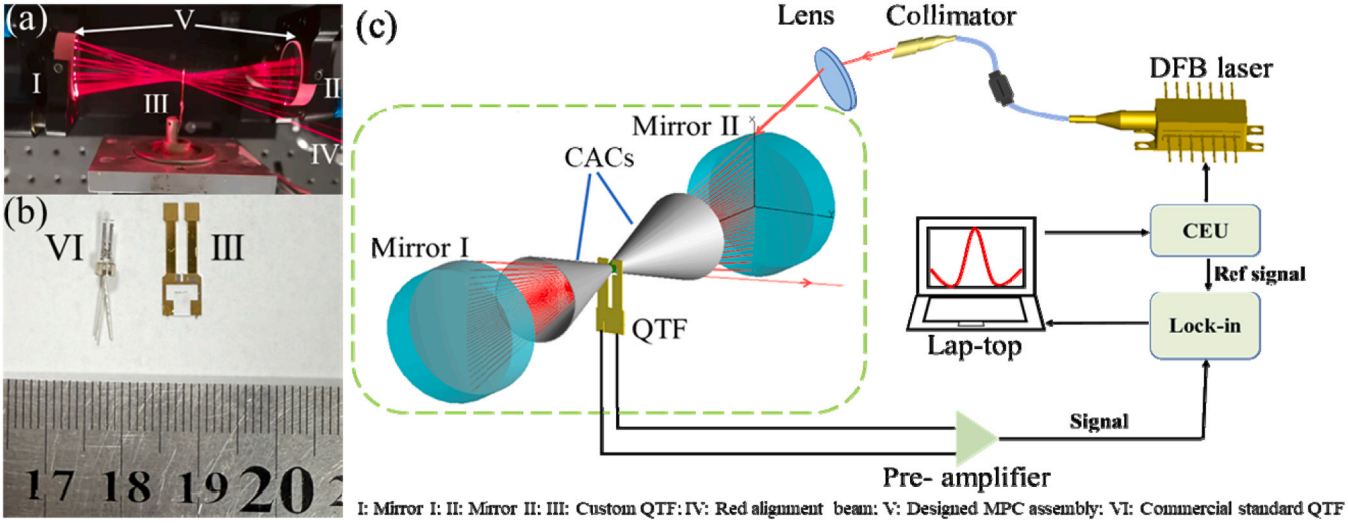

Fig. 3. Experimental setup of the spatially engineered QEPAS configuration. (a) Enlarged photograph of the optical layout showing the MPC and QTF region; the red beam is used only for alignment. (b) Photograph comparing the custom QTF used in this work with a conventional commercial QTF. (c) Schematic of the experimental system incorporating the MPC and CACs.

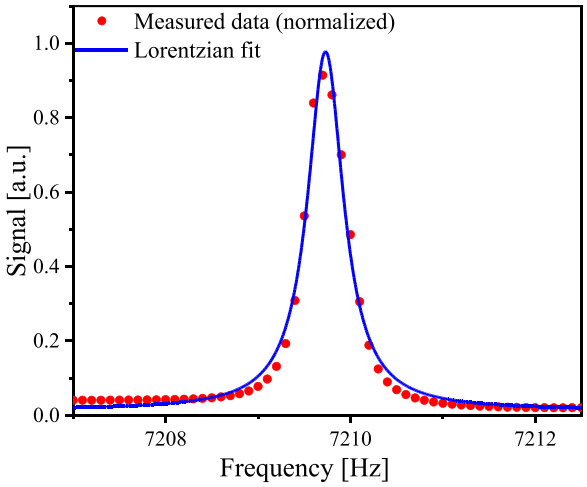

Fig. 4. Normalized frequency response of the custom QTF under electrical excitation, illustrating its intrinsic resonance characteristics. Discrete symbols denote the experimentally measured data, and the solid line represents a Lorentzian fit.

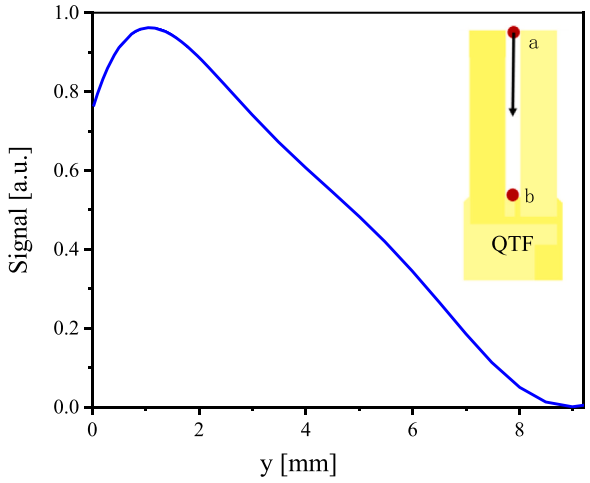

Fig. 5. Normalized QEPAS signal as a function of excitation beam position along the QTF prongs, measured using single-beam excitation. The excitation beam was vertically scanned from the prong tips (point a) toward the prong base (point b), revealing the intrinsic spatial response of the QTF.

reference for evaluating and interpreting enhancement strategies. In particular, it highlights that optical excitation occurring outside this region contributes disproportionately less to the detected signal, even if the total absorbed optical energy is increased.

Based on the spatial response characterization, a baseline measurement was performed using a conventional single-pass QEPAS configuration, in which only a single excitation beam traverses the QTF prong gap. The corresponding second-harmonic ($2f$) photoacoustic spectrum is shown in Fig. 6. Under identical operating conditions, the peak signal amplitude obtained in the single-pass configuration was 0.106 mV. This measurement serves as a reference for assessing the effectiveness of subsequent enhancement schemes. Importantly, in this configuration, the photoacoustic source is spatially localized and only partially utilizes the intrinsic high-sensitivity region of the QTF.

Fig. 6 also compares the $2f$ photoacoustic spectra obtained using MP-QEPAS (MPC only) and QEPAS incorporating both the MPC and CACs. In the MP-QEPAS configuration, multiple excitation beams are folded through the QTF prong gap, with their trajectories spatially confined within the intrinsic high-sensitivity region identified in Fig. 5. The peak signal amplitude increases to 1.44 mV, corresponding to an enhancement factor of approximately 13.6 relative to the single-pass QEPAS configuration. This enhancement can be attributed to the increased number of photoacoustic sources generated within the effective response region of the QTF. It is worth noting that the measured enhancement (~13.6) does not scale strictly with the nominal number of traversals (~20), because the optical power of different passes is not identical due to cumulative MPC losses. In addition, as implied by the QTF spatial-response map in Fig. 5, residual spatial-response weighting and non-identical acoustic coupling of the spatially distributed sources can further reduce the effective contribution of some passes. Unlike conventional MP-QEPAS schemes, where optical absorption may be distributed over regions with suboptimal sensitivity, the present configuration ensures that each excitation pass contributes effectively to the detected signal. These results demonstrate that extending the optical path length alone is insufficient to explain the observed enhancement. Instead, the key factor is the spatial confinement of optical absorption to the QTF intrinsic sensitivity region, which maximizes the transduction efficiency of the generated photoacoustic waves.

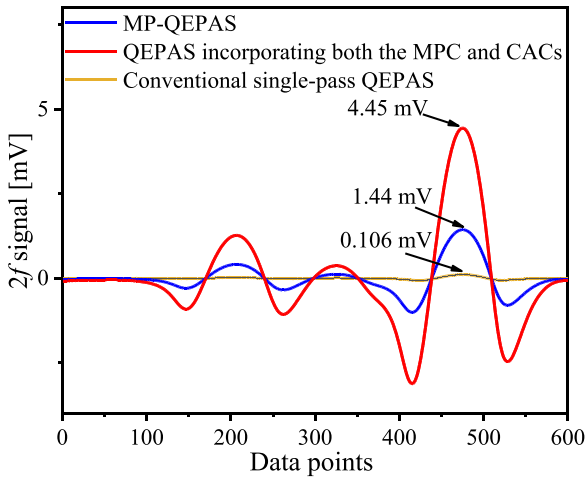

Fig. 6. 2f photoacoustic spectra of 8500 ppm H_2O measured using (i) conventional single-pass QEPAS, (ii) MP-QEPAS (MPC only), and (iii) the spatially engineered QEPAS configuration incorporating both the MPC and CACs. The peak signal amplitudes (0.106 mV, 1.44 mV, and 4.45 mV) are labeled on the corresponding curves. The x-axis denotes the acquisition-point index during the laser scan.

When the CACs are further introduced, the peak signal amplitude increases to 4.45 mV, as shown in Fig. 6. Compared with the MPC-only configuration, this represents an additional enhancement factor of approximately 3.1. Corresponding simulations comparing the MPC configuration with and without CACs predict an acoustic pressure enhancement of approximately 3.4 times at the QTF location, which is in close agreement with the experimentally observed signal increase (~3.1 times). Relative to the conventional single-pass QEPAS configuration, the overall enhancement factor reaches approximately 42. This additional enhancement arises from the efficient collection and guidance of the spatially distributed photoacoustic waves generated by the confined multi-pass excitation. Owing to their conical geometry, the acoustic collectors provide a gradual spatial compression of sound energy toward the QTF prong gap, which is geometrically compatible with the fan-shaped distribution of photoacoustic sources. In contrast to frequency-selective acoustic resonators, this geometry-based collection mechanism operates over a broad bandwidth and does not rely on precise resonance matching. The combined effect of spatially confined optical excitation and geometry-matched acoustic collection confirms that effective spatial overlap between the photoacoustic source volume and the QTF intrinsic sensitivity region governs the achievable signal enhancement. Enhancing either the optical excitation or acoustic coupling alone is insufficient to fully exploit the QTF response when spatial mismatch persists. Unlike the dual-antinode and dual-beam excitation scheme combined with dual acoustic micro-resonators reported in Ref. [39], the present work emphasizes spatial optical–acoustic matching by confining multi-pass absorption to the intrinsic high-response zone of the QTF and using broadband geometric collectors for distributed sound-energy collection.

In addition to the amplitude comparison, we assessed the overall sensing performance using the signal-to-noise ratio (SNR), defined as the peak 2f amplitude divided by the 1σ standard deviation of the baseline noise obtained under the same measurement settings. Relative to the conventional single-pass QEPAS configuration, the SNR increases by approximately a factor of 10 for MP-QEPAS (MPC only) and by approximately a factor of 30 for the configuration incorporating both the MPC and CACs.

From a broader perspective, these results highlight a fundamental limitation of many previously reported QEPAS enhancement schemes, in which optical absorption and acoustic detection are optimized independently. The present study demonstrates that spatial matching constitutes a distinct and critical design dimension, complementary to optical path length extension and acoustic resonance enhancement. By explicitly engineering both the generation and collection of photoacoustic waves to match the intrinsic spatial response of the QTF, substantial signal enhancement can be achieved without relying on narrowband resonance effects or stringent alignment requirements. This spatially engineered optical–acoustic matching strategy provides a robust and general framework for improving QEPAS performance and can be readily extended to other QTF geometries, excitation wavelengths, and multi-beam configurations.

5. Conclusion

In this work, we have demonstrated a spatially engineered enhancement strategy for QEPAS by explicitly matching the optical excitation and acoustic energy collection to the intrinsic spatial response of the QTF. Unlike conventional enhancement approaches that primarily focus on increasing optical path length or acoustic resonance strength, the proposed method addresses the spatial mismatch between distributed photoacoustic sources and the QTF sensitivity profile. By employing a spatially confined multi-pass optical configuration, optical absorption is restricted to the finite high-sensitivity region of the QTF, ensuring that all excitation passes contribute effectively to signal generation. In parallel, geometry-matched conical acoustic collectors are introduced to efficiently collect and guide the spatially distributed photoacoustic waves toward the QTF prong gap without relying on narrowband resonance effects. The coordinated optical–acoustic spatial matching significantly improves the effective utilization of the QTF response region while maintaining alignment tolerance and experimental robustness. The experimental results obtained from water vapor detection under ambient conditions confirm that spatial matching constitutes a critical and previously underappreciated dimension in QEPAS enhancement. More broadly, this study demonstrates that spatial engineering of photoacoustic excitation and detection provides a general and practical framework for improving QEPAS performance beyond specific optical or acoustic implementations. Owing to its conceptual simplicity and geometric nature, the proposed approach can be readily extended to other QTF designs, excitation wavelengths, and multi-beam configurations, offering new opportunities for high-sensitivity and field-deployable photoacoustic gas sensing.

CRediT authorship contribution statement

Yingzhang Ren: Validation, Software. **Chunxia Li:** Validation, Data curation. **Chenglong Wang:** Software, Data curation. **Wenfei Han:** Validation, Software. **Ruyue Cui:** Writing – original draft, Validation, Software, Methodology, Investigation, Funding acquisition, Formal analysis, Data curation. **Lei Dong:** Writing – review & editing, Supervision, Methodology, Funding acquisition. **Hongpeng Wu:** Writing – review & editing, Supervision. **Weidong Chen:** Supervision. **Vincenzo Spagnolo:** Investigation. **Jiale Xu:** Validation, Software. **Xinran Li:** Validation, Software.

Declaration of Competing Interest

The authors declare that they have no known competing financial interests or personal relationships that could have appeared to influence the work reported in this paper.

Acknowledgements

The project is sponsored by National Key R&D Program of China (No. 2025ZD1200704); National Natural Science Foundation of China (NSFC) (Nos. 62505163, 62235010, 62501370, 62475137, 62405042); Fundamental Research Program of Shanxi Province, China (Nos. 202403021212183, 202303021222034); Scientific and Technological

Innovation Programs of Higher Education Institutions in Shanxi Province of China (No. 2024L014); Research Project Supported by Shanxi Scholarship Council of China (No. 2025–060); Shanxi Provincial Special Fund for Scientific and Technological Cooperation and Exchange (202404041101022, 202304041101019).

Data availability

Data will be made available on request.

References

[1] B. Li, X. Yang, Z. Sun, J. Wang, P. Zheng, X. Yin, Low-cost hydrogen sensor with the transient response of a quartz tuning fork, Sens. Actuators B Chem. 443 (2025) 138317.
[2] R. Cui, H. Wu, F.K. Tittel, V. Spagnolo, W. Chen, L. Dong, Folded-optics-based quartz-enhanced photoacoustic and photothermal hybrid spectroscopy, Photoacoustics 35 (2024) 100580.
[3] L. Liu, H. Huan, X. Zhang, L. Zhang, J. Zhan, S. Jiang, X. Yin, B. Chen, X. Shao, X. Xu, A. Mandelis, Wavelength-modulated photoacoustic spectroscopic instrumentation system for multiple greenhouse gas detection and in-field application in the Qinling mountainous region of China, Photoacoustics 38 (2024) 100620.
[4] R. Cui, Y. Yuan, S. Qui, W. Han, J. Huang, L. Wang, H. Wu, W. Chen, L. Dong, Miniaturized 3D-printed multipass helmholtz photoacoustic sensors for high-sensitivity CO_2 detection with near-infrared (NIR) diode lasers, Anal. Chem. 97 (25) (2025) 13095–13102.
[5] Y. Cao, R. Wang, J. Peng, K. Liu, W. Chen, G. Wang, X. Gao, Humidity enhanced N_2O photoacoustic sensor with a 4.53 μm quantum cascade laser and Kalman filter, Photoacoustics 24 (2021) 100303.
[6] Z. Wang, Q. Wang, H. Zhang, S. Borri, I. Galli, A. Sampaolo, P. Patimisco, V. Spagnolo, P. Natale, W. Ren, Doubly resonant sub-ppt photoacoustic gas detection with eight decades dynamic range, Photoacoustics 27 (2022) 100387.
[7] S. Qiao, X. Liu, Z. Lang, Y. He, W. Chen, Y. Ma, Quartz-enhanced laser spectroscopy sensing, Light Sci. Appl. 15 (2026) 5.
[8] Y. Wang, Y. He, S. Qiao, X. Liu, C. Zhang, X. Duan, Y. Ma, Fast step heterodyne light-induced thermoelastic spectroscopy gas sensing based on a quartz tuning fork with high-frequency of 100 kHz, Opto-Electron. Adv. 9 (1) (2026) 250150.
[9] S. Qiao, Z. Lang, Y. He, X. Zhi, Y. Ma, Calibration-free measurement of absolute gas concentration and temperature via light-induced thermoelastic spectroscopy, Adv. Photonics 7 (6) (2025) 066007.
[10] S. Zhu, H. Wang, C. Sun, X. Zhao, H. Qi, Y. Xu, C. Li, X. Wang, K. Chen, Fiber-optic photoacoustic gas sensor based on a miniaturized multi-pass cell with an elliptical cross-section, J. Anal. Test. (2025) 1–11.
[11] H. Wang, C. Sun, X. Zhang, Y. Xu, X. Zhao, H. Qi, K. Chen, Hourglass-shaped resonator-based fiber-optic photoacoustic multipass gas sensor, Anal. Chem. 97 (25) (2025) 13715–13723.
[12] Z. Shang, H. Wu, G. Wang, R. Cui, B. Li, T. Gong, G. Guo, X. Qiu, C. Li, L. Dong, Robust and compact light-induced thermoelastic sensor for atmospheric methane detection based on a vacuum-sealed subminiature tuning fork, Photoacoustics 42 (2025) 10069.
[13] C. Zhang, Y. Gao, R. Cui, H. Zhang, J. Tian, Y. Tang, L. Yang, C. Feng, P. Patimisco, A. Sampaolo, V. Spagnolo, X. Yin, L. Dong, H. Wu, Enhancing photoacoustic trace gas detection via a CNN–transformer denoising framework, Photoacoustics 45 (2025) 10075.
[14] X. Shen, Y. Zhang, R. Cui, D. Tian, M. Cheng, P. Patimisco, A. Sampaolo, C. Sun, X. Yin, V. Spagnolo, L. Dong, H. Wu, A sulfur dioxide detection platform based on photoacoustic spectroscopy and a 266.22 nm high-power stabilized LD-pumped solid-state Q-switched laser, Photoacoustics 42 (2025) 100702.
[15] J. Wang, H. Wu, X. Liu, G. Wang, Y. Wang, C. Feng, R. Cui, Z. Gong, L. Dong, Cantilever-enhanced dual-comb photoacoustic spectroscopy, Photoacoustics 38 (2024) 100605.
[16] C. Feng, X. Shen, B. Li, X. Liu, Y. Jing, Q. Huang, P. Patimisco, V. Spagnolo, L. Dong, H. Wu, Carbon monoxide impurities in hydrogen detected with resonant photoacoustic cell using a mid-IR laser source, Photoacoustics 36 (2024) 100585.
[17] W. Wei, K. Zhou, R. Cui, Z. Shang, H. Wu, L. Dong, PMUT enhanced light-induced thermoelastic spectroscopy, Photoacoustics 46 (2025) 100772.
[18] T. Liang, S. Qiao, Y. Chen, Y. He, Y. Ma, High-sensitivity methane detection based on QEPAS and H-QEPAS technologies combined with a self-designed 8.7 kHz quartz tuning fork, Photoacoustics 36 (2024) 100592.
[19] F. Sgobba, A. Sampaolo, P. Patimisco, M. Giglio, G. Menduni, A.C. Ranieri, C. Hoelzl, H. Rossmadl, C. Brehm, V. Mackowiak, D. Assante, E. Ranieri, V. Spagnolo, Compact and portable quartz-enhanced photoacoustic spectroscopy sensor for carbon monoxide environmental monitoring in urban areas, Photoacoustics 25 (2022) 100318.
[20] S. Borri, P. Patimisco, I. Galli, D. Mazzotti, G. Giusfredi, N. Akikusa, M. Yamanishi, G. Scamarcio, P. De Natale, V. Spagnolo, Intracavity quartz-enhanced photoacoustic sensor, Appl. Phys. Lett. 104 (2014) 091114.
[21] V. Spagnolo, P. Patimisco, S. Borri, G. Scamarcio, B.E. Bernacki, J. Kriesel, Mid-infrared fiber-coupled QCL-QEPAS sensor, Appl. Phys. B 112 (2013) 25–33.
[22] A.A. Kosterev, Y.A. Bakhirkin, F.K. Tittel, S. Mcwhorter, B. Ashcraft, QEPAS methane sensor performance for humidified gases, Appl. Phys. B 92 (2008) 103–109.
[23] Y. Ma, Review of recent advances in QEPAS-based trace gas sensing, Appl. Sci. 8 (10) (2018) 1822.
[24] G. Wu, Y. Zhang, Z. Gong, Y. Fan, J. Xing, X. Wu, J. Ma, W. Peng, Q. Yu, L. Mei, A mini-resonant photoacoustic sensor based on a sphere-cylinder coupled acoustic resonator for high-sensitivity trace gas sensing, Photoacoustics 37 (2024) 100595.
[25] B. Sun, T. Wei, M. Zhang, L. Qiao, Z. Ma, A. Sampaolo, P. Patimisco, V. Spagnolo, H. Wu, L. Dong, Optical synchronous signal demodulation-based quartz-enhanced photoacoustic spectroscopy for remote, multi-point methane detection in complex environments, Photoacoustics 43 (2025) 100708.
[26] P. Patimisco, A. Sampaolo, L. Dong, F.K. Tittel, V. Spagnolo, Recent advances in quartz enhanced photoacoustic sensing, Appl. Phys. Rev. 5 (2018) 011106.
[27] H. Wu, L. Dong, H. Zheng, Y. Yu, W. Ma, L. Zhang, W. Yin, L. Xiao, S. Jia, F. K. Tittel, Beat frequency quartz-enhanced photoacoustic spectroscopy for fast and calibration-free continuous trace-gas monitoring, Nat. Commun. 8 (2017) 15331.
[28] H. Wu, L. Dong, X. Yin, A. Sampaolo, P. Patimisco, W. Ma, L. Zhang, W. Yin, L. Xiao, V. Spagnolo, S. Jia, Atmospheric CH_4 measurement near a landfill using an ICL-based QEPAS sensor with V-T relaxation self-calibration, Sens. Actuators B Chem. 297 (2019) 126753.
[29] N. Petra, J. Zweck, A.A. Kosterev, S.E. Minkoff, D. Thomazy, Theoretical analysis of a quartz-enhanced photoacoustic spectroscopy sensor, Appl. Phys. B 94 (2009) 673–680.
[30] P. Patimisco, G. Scamarcio, F.K. Tittel, V. Spagnolo, Quartz-enhanced photoacoustic spectroscopy: a review, Sensors 14 (4) (2014) 6165–6206.
[31] H. Zheng, L. Dong, H. Wu, X. Yin, L. Xiao, S. Jia, R. Curl, F.K. Tittel, Application of acoustic micro-resonators in quartz-enhanced photoacoustic spectroscopy for trace gas analysis, Chem. Phys. Lett. 691 (2018) 462–472.
[32] L. Dong, A.A. Kosterev, D. Thomazy, F.K. Tittel, QEPAS spectrophones: design, optimization, and performance, Appl. Phys. B 100 (2010) 627–635.
[33] S. Qiao, Y.; He, Y. Ma, Trace gas sensing based on single-quartz-enhanced photoacoustic–photothermal dual spectroscopy, Opt. Lett. 46 (10) (2021) 2449–2452.
[34] Z. Li, Z. Wang, Y. Qi, W. Jin, W. Ren, Improved evanescent-wave quartz-enhanced photoacoustic CO sensor using an optical fiber taper, Sens. Actuators B Chem. 248 (2017) 1023–1028.
[35] H. Wu, A. Sampaolo, L. Dong, P. Patimisco, X. Liu, H. Zheng, X. Yin, W. Ma, L. Zhang, W. Yin, V. Spagnolo, S. Jia, F.K. Tittel, Quartz enhanced photoacoustic H_2S gas sensor based on a fiber-amplifier source and a custom tuning fork with large prong spacing, Appl. Phys. Lett. 107 (2015) 111104.
[36] S. Qiao, Y. Ma, P. Patimisco, A. Sampaolo, Y. He, Z. Lang, F.K. Tittel, V. Spagnolo, Multi-pass quartz-enhanced photoacoustic spectroscopy-based trace gas sensing, Opt. Lett. 46 (5) (2021) 977–980.
[37] Z. Feng, C. Sima, T. Li, W. Wang, Y. Pan, L. Wang, Z. Ming, P. Lu, Highly-sensitive photoacoustic gas sensor with dual resonant modalities for simultaneous NO and NO2 detection, Sens. Actuators B Chem. 434 (2025) 137596.
[38] W. Wang, Z. Feng, Y. Jiang, J. Zhang, S. Yan, X. Cao, P. Lu, C. Sima, Topological optimization method "MMA-BP" for photoacoustic resonator and implementations in ppt-level gas sensor using miniaturized vase-type photoacoustic cells, Photoacoustics 46 (2025) 100767.
[39] H. Zheng, L. Dong, P. Patimisco, H. Wu, A. Sampaolo, X. Yin, S. Li, W. Ma, L. Zhang, W. Yin, L. Xiao, V. Spagnolo, S. Jia, F.K. Tittel, Double antinode excited quartz-enhanced photoacoustic spectrophone, Appl. Phys. Lett. 110 (2017) 021110.
[40] D. Herriott, H. Kogelnik, R. Kompfner, Off-axis paths in spherical mirror interferometers, Appl. Opt. 3 (4) (1964) 523–526.
[41] R. Cui, L. Dong, H. Wu, S. Li, X. Yin, L. Zhang, W. Ma, W. Yin, F.K. Tittel, Calculation model of dense spot pattern multi-pass cells based on a spherical mirror aberration, Opt. Lett. 44 (5) (2019) 1108–1111.

Ruyue Cui received her dual Ph.D. degrees in physics from Shanxi University, China, and Université du Littoral Côte d'Opale, France, in 2023. Currently, she is a lecturer at the Institute of Laser Spectroscopy at Shanxi University. Her research interests encompass optical sensors and laser spectroscopy techniques.

Wenfei Han received her bachelor's degree from Shanxi University, China, in 2024. She is currently pursuing a Master's degree at the Institute of Laser Spectroscopy, Shanxi University. Her research interests include photoacoustic spectroscopy–based sensing technologies.

Chenglong Wang received his B.S. degree in Electrical and Photoelectronic Engineering from West Anhui University, Anhui, China, in 2020, and his M.S. degree in Optoelectronic Engineering from Jinan University, China, in 2024. His research interests include gas sensing technologies, multi-pass cells, tunable diode laser absorption spectroscopy (TDLAS), and photoacoustic spectroscopy.

ChunXia Li is currently pursuing a bachelor's degree in Physics at Shanxi University. Her research interests focus on photoacoustic spectroscopy-based sensing technologies.

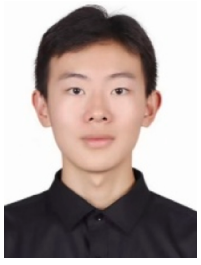

Yingzhang Ren is currently pursuing a bachelor's degree in Optoelectronic Information Science and Engineering at Shanxi University. His research interests include laser spectroscopy and photoacoustic spectroscopy technologies.

Xinran Li is pursuing a bachelor's degree in Optoelectronic Information Science and Engineering at Shanxi University. She has a keen interest in optical sensors and laser spectroscopy techniques

Jiale Xu is currently studying at Shanxi University. She is an undergraduate student majoring in Electronic Information Science and Technology for the class of 2024. Her research interests encompass optical sensors and laser spectroscopy.

Vincenzo Spagnolo obtained the PhD in physics in 1994 from University of Bari. From 1997–1999, he was researcher of the National Institute of the Physics of Matter. Since 2004, he works at the Technical University of Bari, formerly as assistant and associate professor and, starting from 2018, as full Professor of Physics. Since 2019, he is vice-rector of the Technical University of Bari, deputy to technology transfer. He is the director of the joint-research lab PolySense between Technical University of Bari and THORLABS GmbH, fellow member of SPIE and senior member of OSA. His research interests include optoacoustic gas sensing and spectroscopic techniques for real-time monitoring. His research activity is documented by more than 220 publications and two filed patents. He has given more than 50 invited presentations at international conferences and workshops.

Weidong Chen obtained his PhD degree from University of Sciences & Technologies of Lille (USTL) in France. He has been on the faculty at University of the Littoral Opal Coast (France) in 1993 as Lecturer and became full Professor of Optics in 2003. He is adjunct faculty of Rice University (USA) and invited professor of Anhui Institute of Optics and Fine Mechanics (Chinese Academy of Sciences, China). His current research interests include: (1) Developments of photonic instrumentation for applied spectroscopy; (2) Optical sensing and metrology of atmospheric species: trace gases (concentration, isotope ratios, vertical concentration profile) and aerosols (optical properties); (3) Optical parametric laser source generation by frequency conversion. He has authored/co- authored more than 160 peer-reviewed articles in scientific journals, conference proceedings and books. he has over 220 conference contributions (including invited conferences oral and poster presentations) and seminars.

Hongpeng Wu received his Ph.D. degree in atomic and molecular physics from Shanxi niversity, China, in 2017. From 2015–2016, he studied as a joint Ph.D. student in the electrical and computer engineering department and rice quantum institute, Rice University, Houston, USA. Currently he is a professor in the Institute of Laser Spectroscopy of Shanxi University. His research interests include optical sensors and laser spectroscopy techniques.

Lei Dong received his Ph.D. degree in optics from Shanxi University, China, in 2007. From June, 2008 to December, 2011, he worked as a post-doctoral fellow in the Electrical and Computer Engineering Department and Rice Quantum Institute, Rice University, Houston, USA. Currently he is a professor in the Institute of Laser Spectroscopy of Shanxi University. His research activities research activities are focused on research and development in laser spectroscopy, in particular photoacoustic spectroscopy applied to sensitive, selective and real-time trace gas detection, and laser applications in environmental monitoring, chemical analysis, industrial process control, and medical diagnostics. He has published more than 100 peer reviewed papers with > 2200 positive citations.

Ruyue Cui[1], Wenfei Han[1], Chenglong Wang, Chunxia Li, Yingzhang Ren, Xinran Li, Jiale Xu
State Key Laboratory of Quantum Optics Technologies and Devices, Institute of Laser Spectroscopy, Shanxi University, Taiyuan 030006, China
Collaborative Innovation Center of Extreme Optics, Shanxi University, Taiyuan 030006, China

Vincenzo Spagnolo
PolySense Lab—Dipartimento Interateneo di Fisica, University and Politecnico of Bari, Bari, Italy

Weidong Chen
Laboratoire de Physicochimie de l'Atmosphère, Université du Littoral Côte d'Opale, Dunkerque 59140, France

Hongpeng Wu*, Lei Dong*
State Key Laboratory of Quantum Optics Technologies and Devices, Institute of Laser Spectroscopy, Shanxi University, Taiyuan 030006, China
Collaborative Innovation Center of Extreme Optics, Shanxi University, Taiyuan 030006, China

* Corresponding authors at: State Key Laboratory of Quantum Optics Technologies and Devices, Institute of Laser Spectroscopy, Shanxi University, Taiyuan 030006, China.
E-mail addresses: wuhp@sxu.edu.cn (H. Wu), donglei@sxu.edu.cn (L. Dong).

[1] These authors contributed equally to this work